AIP | The Journal of Chemical Physics

Detection of “ended” NO recoil in the 355 nm NO 2 photodissociation mechanism

Vilen K. Nestorov and Joseph I. Cline

Citation: The Journal of Chemical Physics **111**, 5287 (1999); doi: 10.1063/1.479806
View online: http://dx.doi.org/10.1063/1.479806
View Table of Contents: http://scitation.aip.org/content/aip/journal/jcp/111/12?ver=pdfcov
Published by the AIP Publishing

JOURNAL OF CHEMICAL PHYSICS VOLUME 111, NUMBER 12 22 SEPTEMBER 1999

COMMUNICATIONS

Detection of ‘‘ended’’ NO recoil in the 355 nm NO_2 photodissociation mechanism

Vilen K. Nestorov and Joseph I. Cline[a]
Department of Chemistry and Chemical Physics Program, University of Nevada, Reno, Nevada 89557-0020

(Received 15 July 1999; accepted 20 July 1999)

Circularly polarized $1+1'$ REMPI with ion imaging detection was used to probe $\boldsymbol{\mu}$–$\mathbf{v}$–$\mathbf{j}$ angular correlations of the NO $(X\,^2\Pi_{1/2,3/2},\ v=0)$ photoproduct from linearly polarized 355 nm photodissociation of NO_2 in a molecular beam. Rotational angular momentum orientation was measured for the NO product, with the sense and magnitude of the orientation depending upon the direction of the NO recoil velocity with respect to the polarization vector of the photolysis light. The rotational orientation is shown to originate from the directionality of the torque responsible for NO rotational motion. The experimentally observed sense of rotation in the plane of the NO_2 parent molecule is consistent with an effective recoil impulse force applied to the N end of the NO product. A preliminary measure of the bipolar moment associated with this orientation for the $j=21.5$ and $j=36.5$ rotational levels gives a value of approximately $\beta_0^2(21)=0.2$. © *1999 American Institute of Physics.* [S0021-9606(99)01236-2]

In the study of the angular momenta that characterize molecular trajectories in a chemical reaction, a molecule having rotational angular momentum *alignment* has a preferred or avoided *plane of rotation*. Measurements of angular momentum alignment have become routine. Angular momentum *orientation* indicates a preferred *sense of rotation* and has only rarely been measured in molecular dynamics experiments.[1]

To specify rotational orientation, one must choose an observation plane. The presence of rotational orientation results from a net asymmetry of the reaction dynamics in that observation plane. Zare *et al.* observed rotational orientation of N_2 scattered from a crystal surface at non-normal incident angles.[2] For this system the observation plane is perpendicular to the surface and contains the incident velocity vector. A second example is the rotational orientation of CN produced in the photodissociation of ICN by circular polarized light.[3–6] In the circularly polarized photodissociation of achiral molecules the most natural observation plane for measuring rotational orientation is perpendicular to the propagation direction of the photolysis light.

Here we report measurements of rotational orientation for the NO $(X,\ v=0)$ product from the *linearly polarized* 355 nm photodissociation of *randomly oriented* NO_2 molecules. This result may seem surprising, since the total system contains no intrinsic helicity or collective asymmetry. Nonetheless, rotational orientation is observed when probing the correlation of NO rotational angular momentum with recoil direction. We show below that this NO rotational orientation originates from asymmetry in the photodissociation mechanism of individual NO_2 molecules: the recoil impulse is preferentially applied to one end of the NO product molecule.

The 355 nm photodissociation of NO_2 is described by

$$NO_2+h\nu\rightarrow NO(X\,^2\Pi_{1/2,3/2})+O(^3P_{0,1,2}),$$

and has been the subject of numerous previous studies.[7–12] The O $^3P_2$ product channel predominates and excited rotational and vibrational levels $(v=0,1)$ of both the $\Omega=\frac{1}{2}$ and $\frac{3}{2}$ spin–orbit states of NO $(X\,^2\Pi)$ are observed.[13] Angular correlation measurements of the NO fragment trajectory show there is a preference for $\mathbf{j}\perp\mathbf{v}$, where $\mathbf{j}$ is the NO angular momentum vector and $\mathbf{v}$ is the recoil velocity vector. This preferred ‘‘cartwheel’’ NO trajectory is expected since the half-collision recoil dynamics are dominated by forces lying in the plane of the three atoms of the NO_2 parent molecule.[9,11,12]

In contrast, the experiment described here is sensitive to the *sense of rotation* of the NO product in the plane defined by the three atoms of NO_2. The experimental technique is a simple variation of a method described in Ref. 14 for REMPI-TOF probing of molecular stereodynamics using circularly polarized probe light. Reference 14 shows how to quantitatively measure a preferred sense of rotation in the half-collision scattering plane using an extension of the widely used semiclassical bipolar harmonic scheme for describing $\boldsymbol{\mu}$–$\mathbf{v}$–$\mathbf{j}$ angular correlations.[15,16] Within this scheme the spectroscopically measurable $\beta_0^2(21)$ bipolar moment describes the preferred sense of rotation, and the reader is referred to Ref. 14 for a detailed discussion and interpretation of this special instance of ‘‘false’’[17] chiral dynamics.

The diagrams in Fig. 1 illustrate how NO rotational orientation can appear in the NO_2 fragmentation dynamics. At 355 nm the absorption transition dipole, $\boldsymbol{\mu}$, lies in the molecular plane and perpendicular to the C_2 axis.[8] The electric

---

[a] Electronic mail: cline@chem.unr.edu

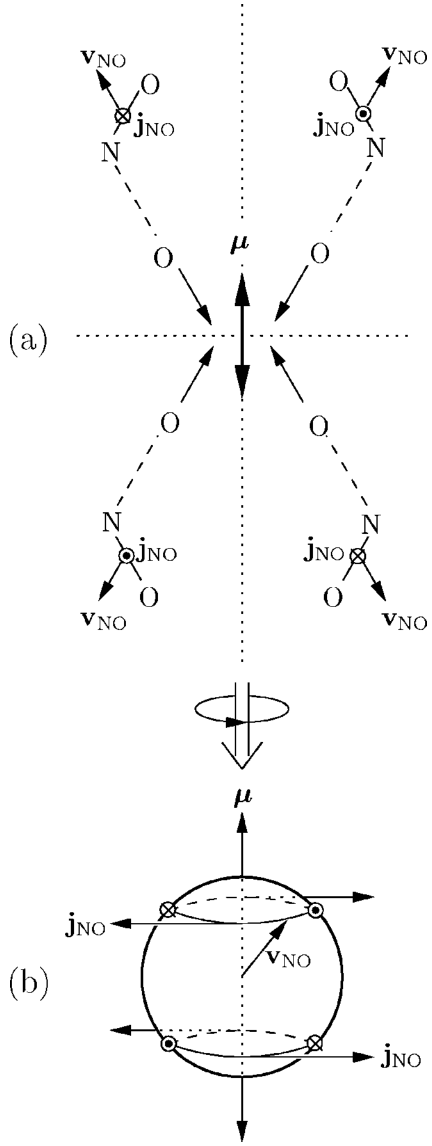

FIG. 1. Diagram (a) depicts the four geometrically distinct transition states for photofragmentation of NO_2, assuming impulsive recoil between the O atom product and the N end of the NO product. In this half-collision scattering plane, the vertical axis is parallel to μ, the NO_2 photodissociation transition dipole. The NO products recoiling into the top left and bottom right quadrants rotate clockwise (**j** directed into the plane), and products recoiling into the top right and bottom left quadrants rotate counterclockwise (**j** directed out of the plane). Diagram (b) shows a three-dimensional representation of the distribution of the NO product trajectories in a frame attached to the $\boldsymbol{\mu}$ vector. The distribution is symmetric about the $\boldsymbol{\mu}$ vector and the tips of the NO recoil velocity vectors, **v**, lie on a sphere. The directions of **j** are tangent to the surface of the velocity sphere and circulate in opposite senses in the upper and lower hemispheres. A $(\hat{\boldsymbol{\mu}}\cdot\hat{\boldsymbol{\epsilon}}_d)^2$ angular distribution of the dynamical objects in (b) is prepared and probed in the experimental measurements.

vector of the linearly polarized photodissociation laser, $\boldsymbol{\epsilon}_d$, preferentially excites NO_2 molecules having C_2 axes perpendicular to $\boldsymbol{\epsilon}_d$. This is depicted in Fig. 1(a) for a single half-collision scattering plane. Let us for the moment suppose the resulting NO product trajectory to be that expected for impulsive recoil of the product O atom from the N end of the NO product. Within this single half-collision scattering plane, there are four ''transition states'' to consider, corresponding to the two possible orientations of NO_2 in the plane and the two possible bonds to be broken. Each of the four cases has a characteristic NO product recoil direction with respect to $\boldsymbol{\mu}$ and a characteristic sense of rotation in the plane of observation. This NO rotational orientation corresponds to **j** directed either into (clockwise rotation) or out of (counterclockwise rotation) the observation plane.

The full, three-dimensional dynamics, and therefore the body-fixed distribution of **v** and **j**, must have cylindrical symmetry about $\boldsymbol{\mu}$. The three-dimensional distribution of the **v**–**j** angular correlation is depicted in Fig. 1(b) by spinning Fig. 1(a) about the $\boldsymbol{\mu}$ axis of symmetry. The resultant recoil velocity sphere in Fig. 1(b) has a radius $|\mathbf{v}|$. The NO angular momentum vector, **j**, produced in coincidence with a particular NO recoil velocity, **v**, is always tangential to the surface of the velocity sphere and always orthogonal to $\boldsymbol{\mu}$. Viewed from a point above Fig. 1(b), the direction of the **j** vector distribution circulates in a clockwise sense in the upper velocity hemisphere, and counterclockwise in the lower hemisphere. This unusual type of $\boldsymbol{\mu}$–**v**–**j** angular correlation corresponds to $0<\beta_0^2(21)\leqslant 1$.[14] If the recoil impulse were instead applied to the O end of the NO product, the sense of circulation of **j** in the two hemispheres would reverse, and $-1\leqslant\beta_0^2(21)<0$.

The experiment to detect the endedness of the photodissociation half-collision was conducted in a molecular beam photofragment ion imaging apparatus similar to those used elsewhere.[18–22] A mixture of 10% NO_2 in He was expanded through a pulsed solenoid valve nozzle. The supersonic expansion passed into the photodissociation chamber through a skimmer and an aperture in a repeller electrode. The molecular beam was orthogonally crossed by the laser beams in a region between the repeller electrode and two aperture electrodes.[23] This stack of electrodes forms an electrostatic ion lens with a symmetry axis along the propagation direction of the molecular beam. The potentials applied to the electrodes were set to the velocity-map focusing condition[23] to create an image on the face of a temporally gated multichannel plate two-dimensional ion detector. Ion images are captured by a CCD camera that is synchronized to the pulsed data acquisition cycle.

The experiment was of the pump-probe type with the rotational orientation of the NO product probed in coincidence with its recoil velocity by two-color $1+1'$ REMPI with ion imaging detection. A data acquisition cycle consisted of a sequence of three laser pulses: (1) a linearly polarized photodissociation pulse at 355 nm with an energy of 9 mJ, (2) a circularly polarized probe laser pulse at ~225 nm with an energy of <100 μJ, and (3) an ionization pulse at 308 nm with a pulse energy of ~1 mJ. The helicity of the circular probe polarization state was alternated between data acquisition cycles using a photoelastic modulator.[24,25]

The ~225 nm probe pulse was circularly polarized and tuned to resolved rotational transitions of the NO $A\,^2\Sigma\leftarrow X\,^2\Pi_{3/2,1/2}$ $(v'=0\leftarrow v''=0)$ band. The 308 nm pulse ionized the NO $(A\,^2\Sigma)$ molecules. for pure *P*- and *R*-branch transitions, the absorption cross section for circularly polarized probe light is sensitive to whether the product molecules are rotating in a clockwise or counterclockwise sense when viewed along the $\mathbf{k}_p$ propagation vector of the probe laser

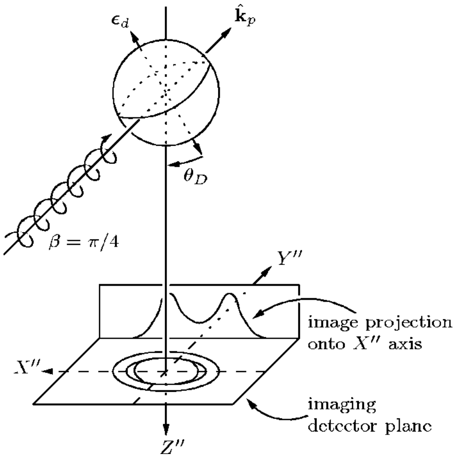

FIG. 2. Experimental geometry for measurement of $\beta_0^2(21)$ by $1+1'$ REMPI with velocity-map ion imaging detection. The molecular beam propagates in the $+Z''$ direction toward the imaging detector and is perpendicularly crossed by laser beams propagating parallel to the Y'' axis. For simplicity, the velocity-map ion optics are not shown, but the symmetry axis of the ion lens is parallel to the Z'' axis. The electric vector of the linearly polarized dissociation light, $\boldsymbol{\epsilon}_d$ is tilted at an angle $0 \leq \theta_D < \pi$ from the Z'' axis, thereby rotating the dynamical object in Fig. 1(b) in the laboratory frame. The circularly polarized probe beam propagation vector, $\mathbf{k}_p$, is in the $+Y''$ direction. The one-dimensional velocity profiles in Fig. 3 are projections of the intensity of the NO^+ velocity-map image onto the X'' axis.

beam. For clockwise rotation, when viewed along the $+\mathbf{k}_p$ direction, the *P*-branch absorption cross section is larger for right-circularly polarized light[26] ($\beta = -\pi/4$) and the *R*-branch absorption cross section is larger for left-circularly polarized light ($\beta = +\pi/4$). The polarization dependence for a pure *Q*-branch transition is nearly insensitive to the sense of rotation.[27]

Figure 2 shows the experimental geometry using the notation from Fig. 1 of Ref. 14. The probe laser propagation direction, $\mathbf{k}_p$, is always perpendicular to the photodissociation laser polarization, $\boldsymbol{\epsilon}_d$. We vary (1) the angle θ_D between the photolysis polarization, $\boldsymbol{\epsilon}_d$, and the symmetry axis of the apparatus, and (2) the helicity of the ~225 nm probe beam. The parameter β is used to characterize the probe helicity, using the convention of Blum.[26,28] By varying θ_D we can project NO products with the same sense of rotation from both the top and bottom halves of the recoil velocity sphere onto the same region of the imaging detector. It can be shown[14,29] that the dependence of the experimental signal on the probe beam helicity is maximum for tilt angles $\theta_D = \pi/4$ and $3\pi/4$. The probe helicity dependence vanishes for $\theta_D = 0$ and $\pi/2$, since any augmentation (depletion) in intensity originating from the top hemisphere is exactly canceled by a depletion (augmentation) originating from the lower hemisphere.

In order to provide a compact representation of the experimental results, we do not show ion images in this Communication, but instead show in Fig. 3 one-dimensional projections of the image data onto the X'' axis of Fig. 2. The one-dimensional projections in Fig. 3 are analogous to REMPI-TOF transitions and contain the essential features necessary to immediately identify the endedness of the NO_2 photodissociation half-collision. A more complete analysis is deferred for future publication.[30] Figure 3 shows projections measured with circularly polarized probing on three selected rotational transitions of the NO product and at four values of the photolysis polarization direction, θ_D. For a given probe helicity, the dependence of the shape of the projections on θ_D is a consequence of ordinary photofragment recoil anisotropy and is consistent with the known preference for $\mathbf{v} \| \boldsymbol{\mu}$ angular correlation arising from the ${}^2B_2 \leftarrow {}^2A_1$ transition of NO_2 at 355 nm.[8,9] The variation in the velocity width of the projections is due to simple conservation of energy constraints.

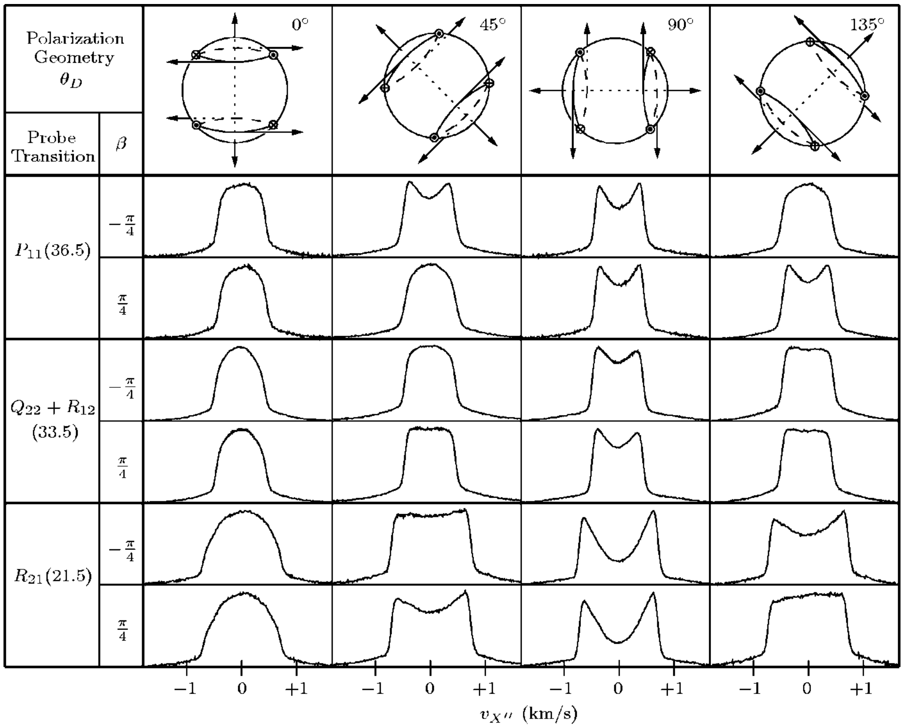

FIG. 3. One-dimensional velocity projections of the measured NO^+ recoil velocity-map image intensity onto the X'' axis in Fig. 2. Projections are shown when probing the NO product $P_{11}(36.5)$, $Q_{22}+R_{12}(33.5)$, and $R_{21}(21.5)$ transitions of the $A \leftarrow X$, $v = 0$ band. The shape of the profiles depends on the photolysis polarization angle, θ_D, the probe helicity, and the branch type, as described in the text. The probe helicity is specified by the helicity parameter β.[26]

Our interest here is in how the velocity projections depend on the probe helicity when probing *P*- or *R*-branch transitions at $\theta_D=\pi/4$ or $3\pi/4$, the two polarization geometries most sensitive to the $\beta_0^2(21)$ bipolar moment. In these instances a projection has either a convex or concave peak, depending on the probe helicity. This results from selective detection of the clockwise (or counterclockwise) rotating NO products concentrated at the center (or periphery) of the projection at these two geometries. Any helicity dependence is exactly opposite for the $\theta_D=\pi/4$ and $3\pi/4$ geometries, since this change in geometry exchanges the locations of the clockwise and counterclockwise NO rotors in the velocity projection. As expected, the probe helicity dependence is also opposite for the P_{11} and R_{21} branch transitions, and negligible for the $Q_{22}+R_{12}$ branch transition.[27] At the $\theta_D=0$ and $\pi/2$ polarization geometries no probe helicity dependence is observed. A preliminary analysis of the images obtained probing the $P_{11}(36.5)$ and $R_{21}(21.5)$ transitions in Fig. 3 gives $\beta_0^2(21)=0.2$, measured by direct fit to imaging theory for polarized $1+1'$ REMPI probing.[29–31] The positive value of $\beta_0^2(21)$ indicates that the N end of the NO product receives the recoil impulse.

Though this result is in accord with the expectations for a simple, classical impulsive photodissociation mechanism for NO_2, the actual mechanism is likely much more complex.[11] The observed sense of rotation is consistent with NO rotation evolving from a decreasing NO_2 bond angle at the instant of bond rupture. Opposite senses of rotation might instead be expected for an alternative fragmentation mechanism in which the NO_2 bond angle increases as a N–O bond ruptures, in which case the O end of NO would effectively receive the recoil impulse.

There is an important relationship between the oriented rotational motion of NO from linearly polarized photodissociation of NO_2 and the oriented electronic angular momentum of the Cl $^2P_{3/2}$ atom from the linearly polarized photodissociation of ICl, recently reported by Rakitzis *et al.*[32,33] The experimental manifestation of the orientation in the two systems is similar,[6,34] but has very different mechanistic origins. In the ICl experiments, the Cl atom electronic orientation arises from quantum mechanical coherence between dissociation channels involving parallel and perpendicular excited states. In the NO_2 experiment the origin of rotational orientation is evident in an intuitive classical picture of the photodissociation recoil trajectory.

We conclude by noting that measurements of this type of rotational orientation can provide detailed mechanistic information for other systems exhibiting prompt photodissociation or for bimolecular scattering.[35]

We thank Dr. K. Thomas Lorenz and Dr. David W. Chandler for numerous contributions and advice in the construction and operation of the ion imaging apparatus at Nevada, and Dr. Gregory E. Hall for helpful discussions. We thank the National Science Foundation for support of this research.

[1] More quantitatively, angular momentum alignment is related to the quadrupole moment of the **j** distribution about a quantization axis. Angular momentum orientation is related to the dipole moment. In a quantum mechanical description the terms refer to the properties of the m_j distribution; see Refs. 36 and 37.

[2] G. O. Sitz, A. C. Kummel, R. N. Zare, and J. C. Tully, J. Chem. Phys. **89**, 2572 (1988).

[3] E. Hasselbrink, J. R. Waldeck, and R. N. Zare, Chem. Phys. **126**, 191 (1988).

[4] J. F. Black, E. Hasselbrink, J. R. Waldeck, and R. N. Zare, Mol. Phys. **71**, 1143 (1990).

[5] M. L. Costen, S. W. North, and G. E. Hall, J. Chem. Phys. (to be published).

[6] J. A. Beswick and O. Roncero, J. Chem. Phys. **96**, 7514 (1992).

[7] M. Mons and I. Dimicoli, Chem. Phys. **130**, 307 (1989).

[8] M. Mons and I. Dimicoli, J. Chem. Phys. **90**, 4037 (1989).

[9] V. P. Hradil, T. Suzuki, S. A. Hewitt, and P. L. Houston, J. Chem. Phys. **99**, 4455 (1993).

[10] A. Sanov, C. R. Bieler, and H. Reisler, J. Phys. Chem. **99**, 13637 (1995).

[11] S. A. Reid and H. Reisler, J. Phys. Chem. **100**, 474 (1996).

[12] Y. Mo, H. Katayanagi, and T. Suzuki, J. Chem. Phys. **110**, 2029 (1999).

[13] Conservation of energy restricts the $v=0$ NO X product to rotational levels $j\leqslant 41.5$; see Ref. 9.

[14] R. Uberna, R. D. Hinchliffe, and J. I. Cline, J. Chem. Phys. **103**, 7934 (1995).

[15] R. N. Dixon, J. Chem. Phys. **85**, 1866 (1986).

[16] R. J. Gordon and G. E. Hall, Adv. Chem. Phys. **94**, 1 (1996).

[17] L. D. Barron, Chem. Phys. Lett. **123**, 423 (1986).

[18] A. J. R. Heck and D. W. Chandler, Annu. Rev. Phys. Chem. **46**, 335 (1995).

[19] P. L. Houston, Acc. Chem. Res. **28**, 453 (1995).

[20] P. Samartzis, I. Sakellariou, T. Gougousi, and T. N. Kitsopoulos, J. Chem. Phys. **107**, 43 (1997).

[21] D. H. Parker and A. T. J. B. Eppink, J. Chem. Phys. **107**, 2357 (1997).

[22] M. Kawasaki *et al.*, J. Phys. Chem. **100**, 19853 (1996).

[23] A. T. J. B. Eppink and D. H. Parker, Rev. Sci. Instrum. **68**, 3477 (1997).

[24] R. Uberna, R. D. Hinchliffe, and J. I. Cline, J. Chem. Phys. **105**, 9847 (1996).

[25] J. S. Spasov and J. I. Cline, J. Chem. Phys. **110**, 9568 (1999).

[26] We quantify the probe helicity using the helicity parameter, β, defined by Blum in Ref. 28. The helicity parameters $\beta=-\pi/4$ and $\beta=+\pi/4$ correspond to right and left circularly-polarized probe light, respectively, as defined in Ref. 38.

[27] The spectroscopic branch dependence of circularly polarized probing of rotational orientation can be understood by examining the $h^{(1)}(j)$ geometrical factor that appears in the relevant absorption intensity expression in Eq. (1) of Ref. 14. In the high-*j* limit, $h^{(1)}=1$ for *P* branches, 0 for *Q* branches, and -1 for *R* branches; see Table I of Ref. 36.

[28] K. Blum, *Density Matrix Theory and Applications* (Plenum, New York, 1981).

[29] V. K. Nestorov, R. Hinchliffe, K. T. Lorenz, R. Uberna, D. W. Chandler, and J. I. Cline, in preparation.

[30] V. K. Nestorov and J. I. Cline (in preparation).

[31] Our image fitting and analysis programs are available at http://www.chem.unr.edu/faculty/cline/fimage.

[32] T. P. Rakitzis, S. A. Kandel, and R. N. Zare, J. Chem. Phys. **108**, 8291 (1998).

[33] T. P. Rakitzis *et al.*, J. Chem. Phys. **110**, 3351 (1999).

[34] The $\beta_0^2(21)$ bipolar moment of Ref. 14 is identical (within a scaling factor) to the $\mathrm{Im}[a_1^{(1)}(\parallel,\perp)]$ term defined by T. P. Rakitzis and R. N. Zare, J. Chem. Phys. **110**, 3341 (1999); G. E. Hall (private communication).

[35] G. M. McClelland and D. R. Herschbach, J. Phys. Chem. **981**, 5509 (1987).

[36] C. H. Greene and R. N. Zare, Annu. Rev. Phys. Chem. **33**, 119 (1982).

[37] R. N. Zare, *Angular Momentum* (Wiley, New York, 1988).

[38] W. A. Shurcliff and S. S. Ballard, *Polarized Light* (Van Nostrand, Princeton, NJ, 1964).